Research on Pneumatic Servo Control for Double-Cylinder Collaborative Loading Based on Neural Network

Xu Jianqiang[*]

Department of Mechanical and Electrical Engineering, Beijing Vocational College of Labor and Social Security, and Beijing Experimental Technical School, No.5, Huixindong Street, Chaoyang District, Beijing, 100029, China

Abstract: The pneumatic control system for double-cylinder collaborative loading is extensively applied in the industry. However, compared to the hydraulic system, it is difficult for the pneumatic system for double-cylinder collaborative loading to get satisfactory effect due to strong non-linearity and low rigidity. To improve robustness of the double-cylinder collaborative loading system and increase its control precision, the double-looped PID hybrid controller and double-variable neural network PDI controller are designed. The comparative test is performed for them in research. The research results indicate that the neutral network control is strongly adaptive to the unknown, uncertain and non-linear features of the controlled objects, can effectively overcome unfavorable influences of the non-linear factors on the system, and improve the control quality.

Keywords: Pneumatic, double cylinder, collaborative loading, servo control, PID, neural network.

1. INTRODUCTION

As one manner of the pneumatic force servo control, the double-cylinder pneumatic collaborative loading is extensively applied. Generally the double-cylinder collaborative loading system indicates the position loading system in most cases. The load motion is out of control in this system. The force is uniquely controlled. The focus is to solve the multi-residual force elimination problem in research, so this problem belongs to single-variable control system.

The double-cylinder collaborative loading studied in this paper is different from the above position loading system and belongs to the double-cylinder motion collaborative loading control system. When this system works, the motion speed of the load and clamping force of double cylinders on the load should be controlled simultaneously when the system is working, namely the load force and motion speed are controlled. This system belongs to double-variable control system. The left and right cylinder will move while imposing the force on the load in control. The load force should change according to the given law and the load should move along the given speed curve. It is complex to control the double-cylinder motion collaborative loading system and the main problem is to solve the mutual coupling problem of double variants and influence of different non-linear control factors of the system on control.

2. ESTABLISHMENT OF DOUBLE-CYLINDER LOADING SYSTEM

2.1. System Scheme

The block diagram of the double-cylinder motion collaborative loading experimental system is shown as the Fig. (**1**). This system is the pneumatic servo control system for the double closed-loop valve-controlled cylinder and an industrial computer is used to control and monitor the pneumatic loading in real time. The system includes the load force control closed-loop circuit and speed control closed-loop circuit. The control components include the proportional pressure valve and proportional direction vale. The executive components include the loading cylinder and main pneumatic cylinder. The load is clamped by two cylinders. The force sensor is installed on the load to detect the loading force on the load. The speed sensor is installed on the master cylinder to detect the motion speed of the cylinder piston rod, namely load motion speed. The control variant includes the loading force F of the load and motion speed V of the load.

When the system is operating, the computer will perform double-cylinder collaborative control over the master cylinder and loading cylinder. The speed control force should be coordinated with the force control. The master cylinder should be coordinated with the loading cylinder. The motion law of the controlled objects should be ensured and the force law of the controlled object should be also ensured, so the double-variant control of the load force and motion is realized. The loading cylinder is used to complete the force control experiment and provide the external force load for position control and speed control
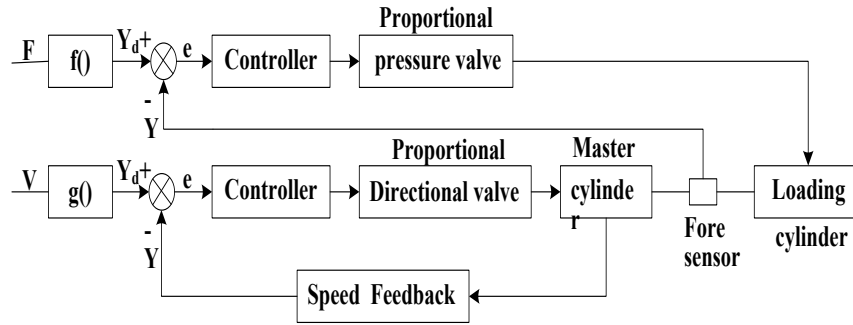
Fig. (1). Electric Servo Control System of Double Closed-loop Valve-controlled Cylinder.
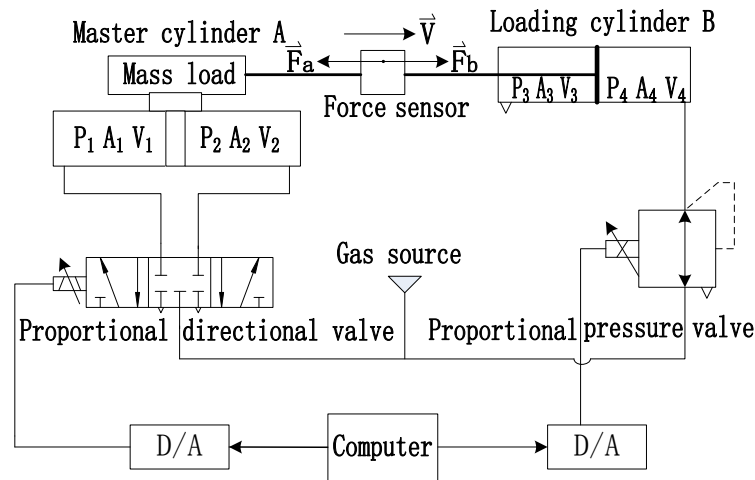
Fig. (2). Structure Schematic of Double-cylinder Collaborative Force Servo Loading Experimental System.

experiment. The master cylinder can be used to complete position control and speed control experiment and assist the loading cylinder to complete the force loading control experiment.

2.2. System Structure

The structure of the double-cylinder motion collaborative loading experimental system [1] is show as the Fig. (2). This system includes the pneumatic device and detection control device. The pneumatic device includes the proportional directional valve, proportional pressure valve, rod cylinder (loading cylinder), rod-less cylinder (master cylinder) and different accessories. The detection control device includes the industry control computer, shift sensor, force sensor, signal conditioning circuit and control software.

The cylinder in the speed control circuit (called as master cylinder) should be low-friction rod-less cylinder, which features high stability, big rigidity, strong bearing capability, low friction and symmetric two-cavity feature and is suitable for research on speed and position servo

control. The DGP-40-600-PPV-A-B from Germany FES-TO cylinder is selected in this system. The cylinder diameter is 40mm and the stroke is 600mm.

The loading cylinder and load cylinder (namely rodless cylinder) will collaboratively move in double-cylinder collaborative loading control, so the structural parameters of the loading cylinder should be similar to it of the master cylinder. Single piston rod double-action cylinder produced by Japan SMC is selected in this system according to the structure requirement. The model is DNC-50-600-PPV-A. The cylinder strake is 600mm and the diameter is 50mm.

The control valve in the speed closed-loop control circuit should be a pneumatic servo valve with the low power consumption, high dynamic response frequency and electric feedback function. The MPYE proportional directional valve from Festo is preferred in this system according to the performance requirements.

The control valve in the load force closed-loop control circuit should be a proportional pressure valve with better dynamic performance, embedded feed-back circuit and better linearity. The VEP3121-1 electric proportional
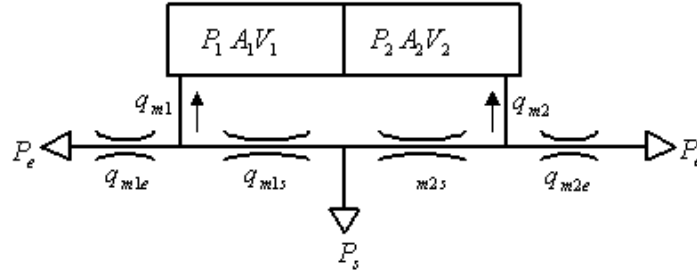
Fig. (3). Equivalent Flow Graph of Proportional Directional Valve-controlled Cylinder Model.

pressure valve produced by Japan SMC is selected in this system.

2.3. Software Design [2]

The Lab Windows/CVI software development platform is used to develop the system control program under Windows environment. This software can perform data collection, data analysis, data display and real-time control for the system. The corresponding control functions are divided into different modules in development of the control program, e.g. collection program, data processing program, display program, output control program, human-machine contact program, and then the program modules are developed.

The double-thread structure is used in program design. The main thread can realize parameter setup, control method selection, OS command and signal source generation functions. The secondary thread can realize data collection, digital filtering, control algorithm and control output functions.

3. MATHEMATIC MODEL OF SYSTEM[3]

E.g. for the motion of the system load from left to right, the double-cylinder collaborative loading system is dynamically analyzed to establish a mathematical model.

Shown as the Fig. (**2**), the master cylinder (rod-less cylinder) is assumed as cylinder A and the load cylinder (rod cylinder) is assumed as the cylinder B.

3.1. Dynamic Description of Cylinder A

The equivalent flow graph of the proportional directional valve-controlled cylinder model is shown as the Fig. (**3**).

Shown as the Fig. (**3**), the mass flow flowing into valve's two cavities is described as follows:

$$q_{mi} = q_{mis} - q_{mie} \tag{1}$$

Mass flow equation at the valve port:

$$q_{miq} = C_d A_q \cdot \frac{p_H}{\sqrt{RT_H}} \cdot f\left(\frac{p_D}{p_H}\right) \tag{2}$$

Dynamic equation of valve port:

$$\dot{p}_i V_i + p_i \dot{V}_i k = km_i RT_i \tag{3}$$

Based on the equation (1) and (3), the pressure change equation of two cavities of cylinder A is obtained as follows:

$$\dot{p}_i = \frac{\frac{kRC_dT_i}{\sqrt{RT_s}}\left[\begin{array}{c} A_{qis}(u) \cdot p_s \cdot f\left(\frac{p_i}{p_s}\right) \\ -\sqrt{\frac{T_s}{T_i}} \cdot A_{qie}(u) \cdot p_i \cdot f\left(\frac{p_e}{p_i}\right) \end{array}\right] - kp_i\dot{V}_i}{V_i} \tag{4}$$

Piston force equation of cylinder A:

$$M_a\ddot{x} = (p_1 - p_2)A_p - B_a\dot{x} - f_{pa}\,\mathrm{sgn}\,\dot{x} - F_a \tag{5}$$

3.2. Dynamic Description of Cylinder B

Force equilibrium equation of Spool in Proportional pressure valve:

$$m_V\ddot{x}_V + B_V\dot{x}_V + K_Sx_V + f_V\,\mathrm{sgn}\,\dot{x}_V = K_{ub}u_b - p_fA_f \tag{6}$$

Position force equilibrium equation of cylinder B:

$$M_b\ddot{x} = F_b + A_3p_3 - A_4p_4 + p_e(A_3 - A_4) - B_b\dot{x} - f_{pb}\,\mathrm{sgn}\,\dot{x} \tag{7}$$

Cylinder pressure equation of right cavity of cylinder B:

$$\dot{p}_4 = \frac{k}{V_{40} + \frac{1}{2}A_4S_b - A_4x}\left(RT_4\frac{C_dA_qp}{\sqrt{RT}}\phi(z) - p_4A_4\dot{x}\right) \tag{8}$$

3.3. System State Equation [4]

1) State variable:

$$x_1 = x,\, x_2 = \dot{x},\, x_3 = x_V,\, x_4 = \dot{x}_V,\, x_5 = p_1,\, x_6 = p_2,\, x_7 = p_4 \tag{9}$$

2) System state equation:

$$\dot{x}_1 = x_2 \tag{10}$$
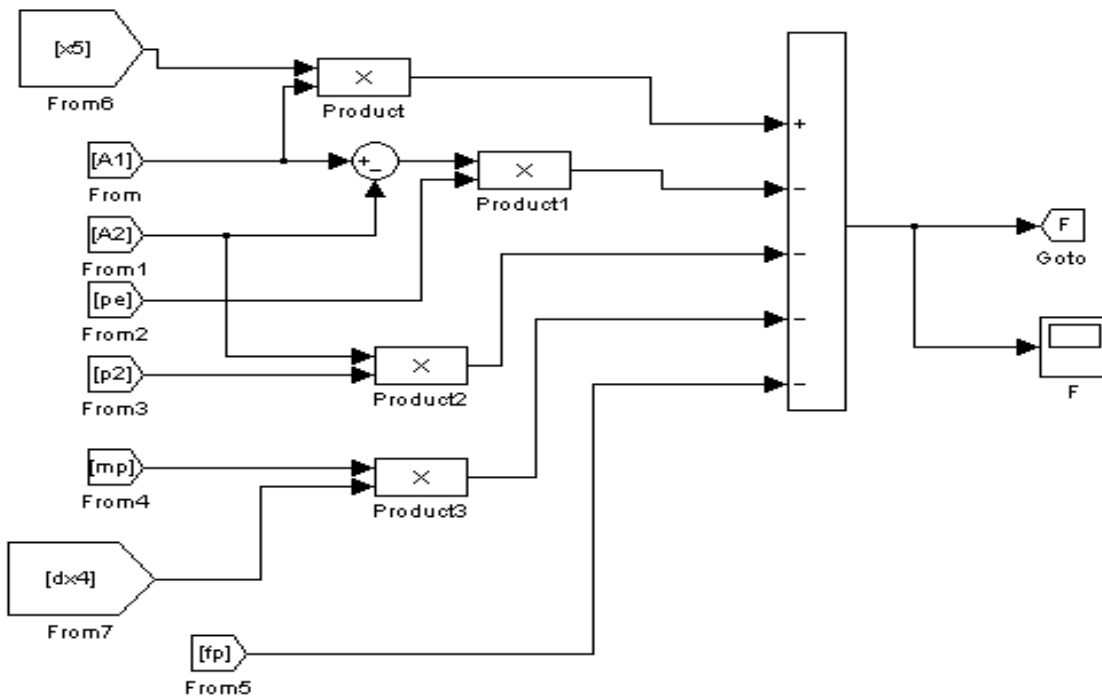
Fig. (4). Output Equation Sub-system Simulation Module Diagram.

$$\dot{x}_2 = \frac{\begin{array}{c}(x_5 - x_6)A_p - (A_4 x_7 - A_3 p_3) + p_e(A_4 - A_3)\\ -(B_a + B_b)x_2 - (f_{pa} + f_{pb})\operatorname{sgn}x_2\end{array}}{M_a + M_b} \quad (11)$$

$$\dot{x}_3 = x_4 \quad (12)$$

$$\dot{x}_4 = \frac{1}{m_V}(K_{ub} \cdot u_b - P_f \cdot A_f - B_V x_4 - K_S x_3 - f_V \operatorname{sgn}x_4) \quad (13)$$

$$\dot{x}_5 = \frac{\frac{kRC_d}{\sqrt{R/T_s}}\left[A_{q_{1s}}(u_a) \cdot p_s \cdot f\left(\frac{x_{51}}{p_s}\right) - A_{q_{1e}}(u) \cdot p_1 \cdot f\left(\frac{p_e}{x_5}\right)\right] - kA_p p_1 x_2}{V_{10} + \frac{1}{2}A_p S_a + A_p x_1} \quad (14)$$

$$\dot{x}_6 = \frac{\frac{kRC_{da}}{\sqrt{R/T_S}}[A_{q2s}(u_a)p_s \cdot f(\frac{x_6}{p_5}) - A_{q2e}(u) \cdot p_2 \cdot f(\frac{p_e}{x_6}) + kA_2 p_2 x_2]}{V_{20} + \frac{1}{2}A_p S_a - A_p x_1} \quad (15)$$

$$\dot{x}_7 = \frac{k}{V_{40} + \frac{1}{2}A_4 S_b - A_4 x_1}(RT_4 \frac{C_{db}A_q p}{\sqrt{RT}}\phi(z) - p_4 A_4 x_2) \quad (16)$$

3) Output: v, F_a or F_b

$$\mathrm{v} = x_2 = \dot{x} \quad (17)$$

$$F_a = (P_1 - P_2)A_P - B_a x_2 - f_{pa}\operatorname{sgn}x_2 - M_a \dot{x}_2 \quad (18)$$

$$F_b = M_b \dot{x}_2 - A_3 p_3 + A_4 x_7 - p_e(A_3 - A_4) + B_b x_2 + f_{pb}\operatorname{sgn}x_2 \quad (19)$$

4) Input u_a and u_b

4. SIMULATION RESULTS AND ANALYSIS [5]

To analyze the system features, the double-cylinder collaborative loading system is simulated under the static state is simulated. The p_1, p_2 and p_4 block are established according to the system state equation (14), (15) and (16) in the system simulation. The inputs include the valve openness and cylinder shift. The outputs include p_1, p_2 and p_4. Based on the equation (13), the system acceleration is obtained. After one-order integral and two-order integral, the system speed and shift can be obtained. After the initial values of seven state variants are set, the state variant value can be computed at any time in the motion simulation. Based on the equation (18), the simulation for the load force F can be performed. The simulation module diagram is shown as the Fig. (**4**). The simulation curve of the system open-loop control and closed-loop control is shown as the Fig. (**5** and **6**).

The transmission medium of the pneumatic control system is the compressed air and its rigidity and stability is worse much than it of the hydraulic medium, so the closed-loop control is used and a proper control method is used to improve the system response. It is difficult to model a nonlinear system, so the modern control theory is difficult to get satisfactory effect. We propose the neural network
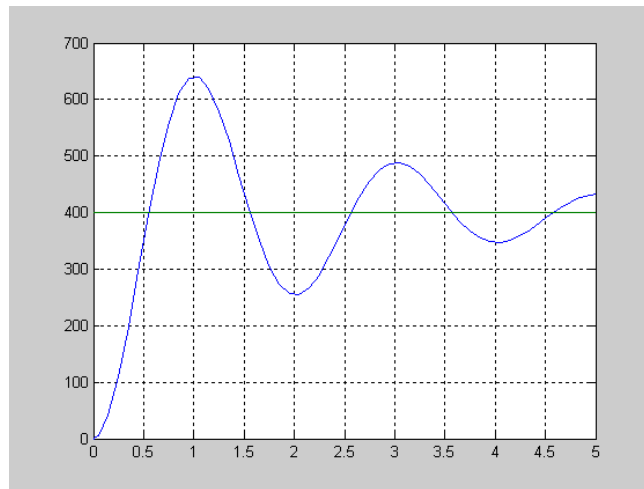
Fig. (5). 400N Step Response Simulation Curve for Open-loop Control.
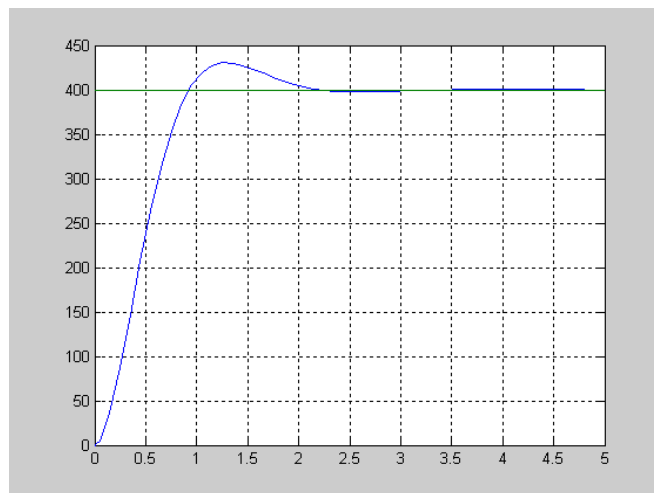
Fig. (6). 400N Step Response Simulation Curve for Close-loop Control.

control strategy to study the pneumatic servo control system for double-cylinder collaborative loading.

5. DESIGN OF DOUBLE-CYLINDER PNEUMATIC FORCE SERVO CONTROLLER BASED ON NEURAL NETWORK PID

5.1. Neural Network Double-Variant Control Structure [6]

To reach better control effect, the double-cylinder pneumatic force servo system is controlled by using the controller based on the neural network and the neural network double-variable control structure is shown as the f Fig. (7).

Assuming that the controlled object of the double-cylinder collaborative loading system is P, which is the double-input double-output (DIDO) system with controlled variant force and speed, the controller NFC includes two PID neural sub-networks. Three neurons at the hidden layer of the sub-network are proportion P, integral I and differential D unit. Assuming that two networks are F and V, each sub-network includes two inputs and one output. One input of the sub-network F corresponds to the given value r_1 of controlled variant force. Another input corresponds to the system output y_1 One input of the sub-network v corresponds to the given value r_2 of the controlled variant speed. Another input corresponds to the system output y_2, u_1 and u_2 are two network outputs v_1, and v_2 are the disturbance imposed on the system output.

This PID neural network is a three-layer forward feedback network consisting of the processing units with the general sigmoid function feature and provides any nonlinear mapping capability from inputs to outputs in L_2
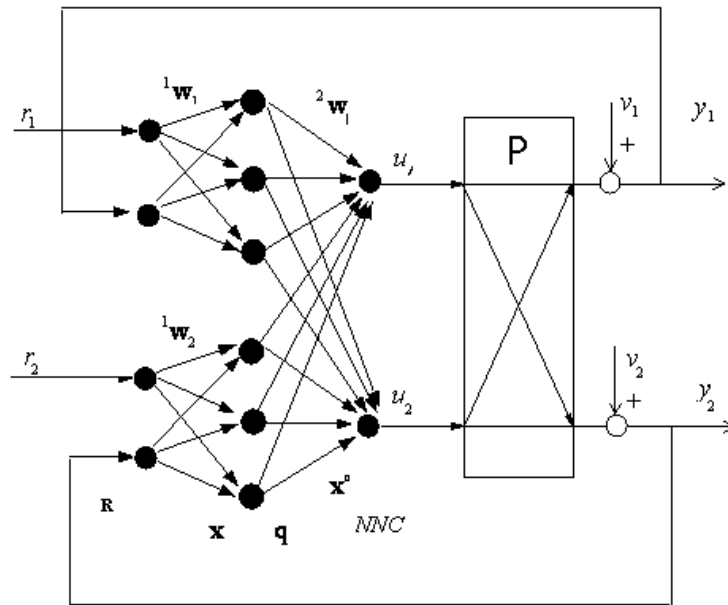
Fig. (7). Neural Network Double-variant Control Structure.

meaning. When BP algorithm is used for learning and training, the mapping from inputs to outputs of the control system (including controlled object) is completed according to the requirements of the rule function $E \rightarrow E_{min}$. The PID neural network makes the decoupling control performance reach the requirement in the weight adjustment training and learning.

5.2. Controller Algorithm [7]

1) Input and output

a. Input and output of the neutrons at the input layer:

$$R = [r_1, y_1, r_2, y_2] = [r_{sj}] \tag{20}$$

s: sub-network SN, s=1, 2:

j: SN of the neutrons at sub-network input layer, $j = 1, 2$

b. Input and output of hidden neutrons

Input of ith node of s sub-network hidden layer:

$$x_{si}(k) = \sum_{j=1}^{2} {}^{1}w_{sij} r_{sj}(k) , \quad i = 1,2,3 \tag{21}$$

Output $q_{si}(k)$ of P, I and D node at s sub-network hidden layer.

$$q_{s1}(k) = \begin{cases} x_{s1}(k) , & -1 \leq x_{s1}(k) \leq 1 \\ 1 , & x_{s1}(k) > 1 \\ -1 , & x_{s1}(k) < -1 \end{cases} \tag{22}$$

$$q_{s2}(k) = \begin{cases} q_{s2}(k-1) + x_{s2}(k) , & -1 \leq q_{s2}(k) \leq 1 \\ 1 , & q_{s2} > 1 \\ -1 , & q_{s2} < -1 \end{cases} \tag{23}$$

$$q_{s3}(k) = \begin{cases} x_{s3}(k) - x_{s3}(k-1) , & -1 \leq q_{s3}(k) \leq 1 \\ 1, & q_{s3} > 1 \\ -1, & q_{s3} < -1 \end{cases} \tag{24}$$

c. Input and output of neutrons at output layer

The input is the weighted sum of outputs of nodes at the hidden layer of two sub-networks:

$$x_1^O(k) = \sum_{s=1}^{n} \sum_{i=1}^{3} {}^{2}w_{s1i} q_{si}(k) \tag{25}$$

$$x_2^O(k) = \sum_{s=1}^{n} \sum_{i=1}^{3} {}^{2}w_{s2i} q_{si}(k) \tag{26}$$

${}^{2}w_{shi}$: weight from the hidden node I to output node h in s^{th} sub-network.

d. Network output:

$$u_1(k) = x_1^O(k) \tag{27}$$

$$u_2(k) = x_2^O(k) \tag{28}$$
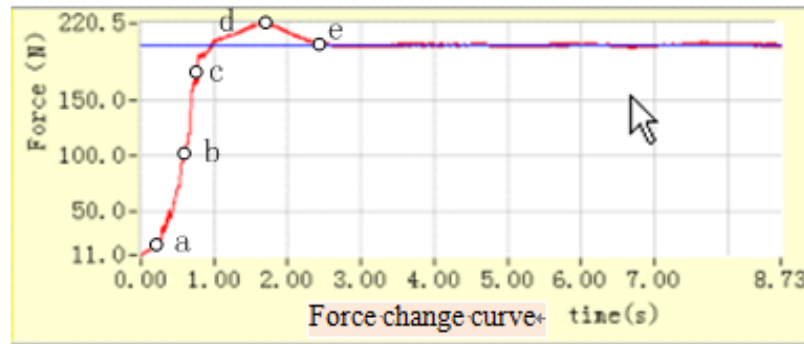
Fig. (8). Force PID Control Step Response Curve.

2) Learning algorithm

The PID neural network controller and multi-variant object are regarded as the general network. The back propagation (BP) learning algorithm is used for online real-time training. The rule function is:

$$J = \sum_{p=1}^{n} E_p = \frac{1}{2}\sum_{p=1}^{n}\left[r_p(k) - y_p(k)\right]^2 = \frac{1}{2}\sum_{p} e^2(k) \tag{29}$$

p: SN of the input variant, which is same as s, p=1,2

a. Weight value adjustment algorithm from hidden layer to output layer after k-step training

$$^2w_{shi}(k+1) = {}^2w_{shi}(k) - \eta_{shi}\frac{\partial J}{\partial^2 w_{shi}}$$

$$= {}^2w_{shi} + \sum_{p=1}^{n}\delta'_{ph}(k)q_{si}(k) \tag{30}$$

$$\delta'_{ph}(k) = e_p(k)\frac{y_p(k) - y_p(k-1)}{u_h(k-1) - u_h(k-2)} \tag{31}$$

b. Weight value adjustment algorithm from input layer to hidden layer after k-step training

$$^1w_{sij}(k+1) = {}^1w_{sij}(k) - \eta_{sij}\frac{\partial J}{\partial^1 w_{sij}}$$

$$= {}^2w_{sij} + \sum_{p=1}^{n}\sum_{h=1}^{n}\delta_{shi}(k)r_{sj}(k) \tag{32}$$

$$\delta_{shi}(k) = \delta'_{ph}(k)({}^2w_{shi})\,\mathrm{sgn}\frac{q_{si}(k) - q_{si}(k-1)}{x_{si}(k) - x_{si}(k-1)} \tag{33}$$

c. Specific implementation steps of algorithm

a) Identify the input/output variants and initialize the weights:

b) Compute the output $u_1(k)$ and $u_2(k)$ of NNC according to the input given value $r_p(k)$ and output sampled value $y_p(k)$

c) Compute the change Δw_{sij} of the weight value according to BP back propagation algorithm and change the weight values of the neutrons.

d) Return to the step b) and perform it.

6. EXPERIMENTAL RESULTS AND ANALYSIS [8]

The comparative experiment results of PID double-variant control and neural network PID double-variant control are shown as follows:

6.1. Comparative Experiment of Step Input Signals

6.1.1. Experimental Conditions

The input signal is the step signal and the given force F=200N and given speed V=40mm/s.

6.1.2. Experimental Results

1) The step response curve of PID control is shown as the Fig. (**8** and **9**):

2) The step response curve of the neural network PID controller is shown as the Fig. (**10** and **11**).

6.1.3. Experimental Analysis

1) Comparative analysis of the step response curve in the Fig. (**8** and **10**)

a. Analysis on overshoot MP: The Fig. (**8**) shows the PID control step response curve. From the coordinate e on the curve, the overshoot peak is 220.5N, the stable value is 200N, and the overshoot value is 10%. The Fig. (**10**) indicates the step response curve of neural network PID control. Its overshot peak is 0 and the response has no overshoot.

b. Analysis on response time t_s. The Fig. (**8**) shows the PID control step response curve. From the coordinate of point e, the response time is 2.4s. The Fig. (**10**) indicates the step response curve of neural network PID control. From the coordinate of point e′, the response time is 1.5s.
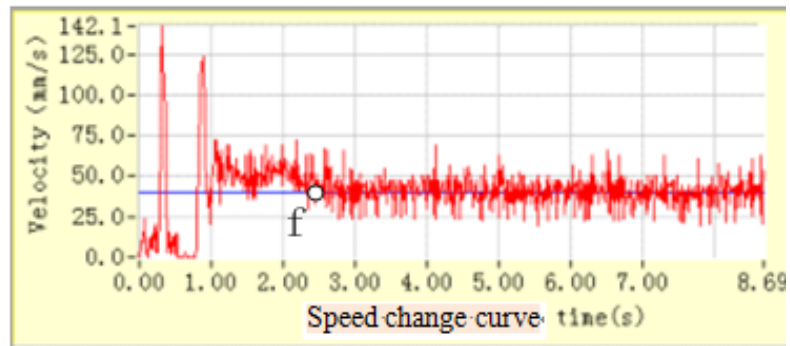
Fig. (9). Speed PID Control Step Response Curve.
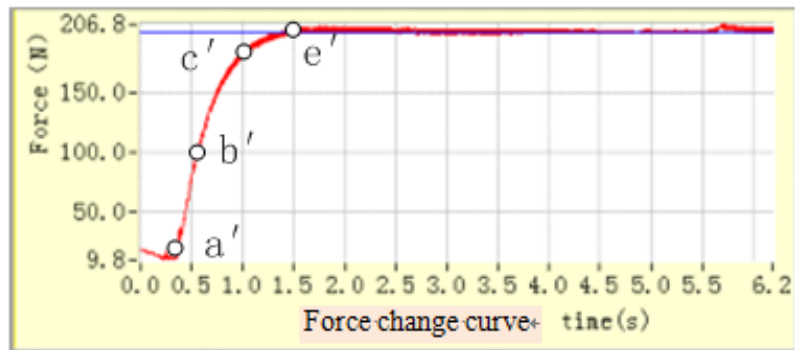
Fig. (10). Force Neural Network PID Control Step Response Curve.
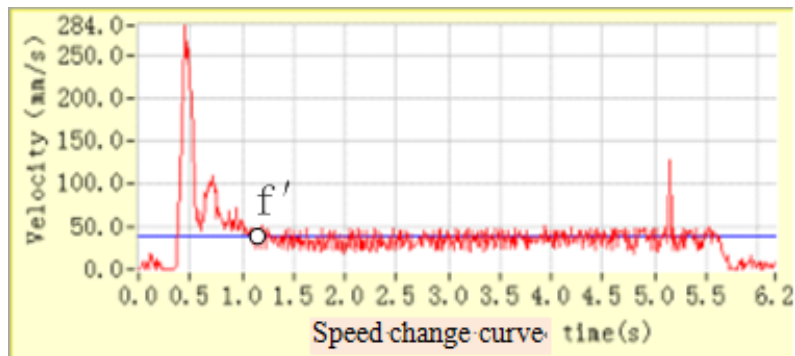
Fig. (11). Speed Neural Network PID Control Step Response Curve.

c. Analysis on ascending time t_r. The Fig. (**8**) shows the step response curve of PID control. From the coordinate of the point a and c. the ascending time is 0.4s. The Fig. (**10**) shows the step response curve of neural network PID control. From the coordinate of the point a′ and c′, the ascending time is 0.7s.

d. Analysis on delay t_d. The Fig. (**8**) shows the step response curve of PID control. From the coordinate of point b, the delay is 0.6s. The Fig. (**10**) shows the step response curve of neural network PID control. From the coordinate of point b′, the delay is 0.6s.

2) Comparative analysis on speed step response curve in the Fig. (**9** and **11**).

a. Analysis on response time: The Fig. (**9**) shows the speed step response curve of PID control. From the coordinate of the point f, the response time is 2.5s. The Fig. (**10**) shows the speed step response curve of neural network PID control. From the coordinate of the point f′, the response time is 1.2s.

b. Analysis on stable state error: the stable state error of the response curve is 25mm/s in the Fig. (**9**). The stable error of the response curve is only 10mm/s in the Fig. (**11**).

The above experimental data indicate that the ANN-PID control system and PID control system have same response speed on the initial phase. Although the ascending time of ANN-PID control system is longer slightly than it
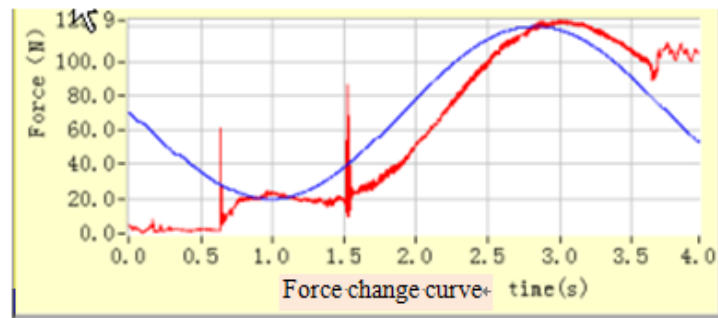
Fig. (12). Force PID Control Sine Response Curve.
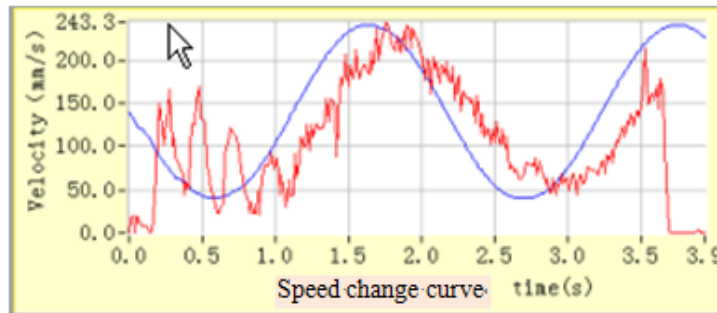
Fig. (13). Speed PID Control Sine Response Curve.
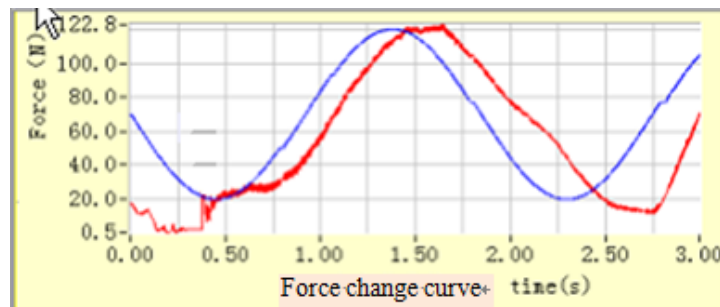
Fig. (14). Force PID Control Cine Response Curve.

of PID control system, the response time of ANN-PID control system is 0.9s less than it of the PID control system. The step response of the ANN-PID control has no overshoot, so it shortens the step response time of the ANN-PID control system, which is caused by intelligent adjustment of the neural network control algorithm. The step response of the ANN-PID control system features first quick and later slow, no overshoot, short response time, and small stable state error, so it improves robustness, accuracy and quickness of the control system.

6.2. Comparative Test of Sine Input Signals

6.2.1. Experimental Conditions

The input signal is Sine signal. The force F is the sine signal with 100N amplitude and 4s cycle. The speed V is the sine signal with 200mm/s amplitude and 2s cycle.

6.2.2. Experimental Results

1) The sine response curve of PID control is shown as the Fig. (**12** and **13**).

2) The sine response curve of neural network PID controller is shown as the Fig. (**12** and **14**).

6.2.3. Experiment Analysis

1) Comparative analysis on force sine response curve in the Fig. (**12** and **14**).

To compare the curve in the Fig. (**12** and **14**), the force output response of ANN-PID control system not only tracks change of the input signals, but also has smoother curve than it of the PID control system.

2) Comparative analysis on speed sine response curve in the Fig. (**13** and **15**).
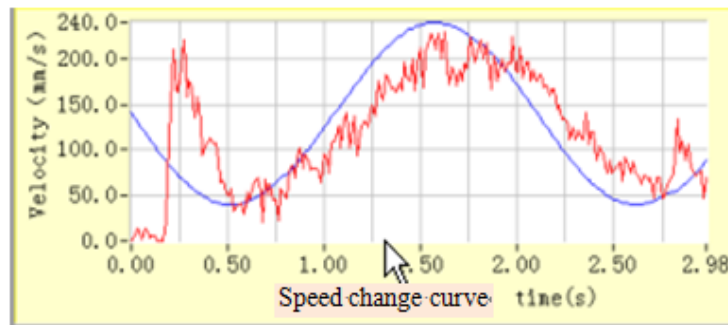
Fig. (15). Speed PID Control Sine Response Curve.

To compare the curve in the Fig. (**13** and **15**), the speed output response of ANN-PID control system not only tracks change of the input signals, but also has the wave form which approaches to the input signals better than it of the PID control system.

3) The curve obtained in the experiment has higher noises because the system uses the simulated shift sensor and the motion speed signals of the cylinder are computed via the differential method. When the cylinder operates at a low speed, the friction is bigger and is not uniform and crawling is easy to occur.

The above analysis results that the neural network control algorithm can effectively weaken influence of the system's non-linear factors and coupling among variants. The response of the ANN-PID control system has no significant lagging compared to it of the PID control system.

CONCLUSION

For the strong non-linearity and low rigidity of the pneumatic force servo system, this paper proposes the neural network control strategy and designs the double closed-loop PID hybrid controllers and double-variant neural network PID controller for comparative experimental research. The experimental research indicates that the object model need not be known and the system need not be identified in system control based on a neural network, so this method is suitable for control over the strong non-linear and uncertain unknown system without accurate model. Better effect is achieved in the research experiment for the pneumatic force servo control system. The pneumatic force servo control system can improve the system robustness and control precision in case of double-cylinder collaborative low-speed motion loading.

CONFLICT OF INTEREST

The authors confirm that this article content has no conflicts of interest.

ABOUT AUTHOR

Xu Jianqiang (1965-), male, be born in Beijing of China, master of engineering, majoring in Mechanical manufacturing and automation specialty of Xi'an Jiaotong University, an associate professor of Beijing Labor and Social Security Vocational College and Beijing Experimental Technical School, and be interested in research on fluid control and computer control.

REFERENCES

[1] Zhao Hong, "Research on Control Strategy of Pneumatic Nonlinear System and Its Application", Ph. D. thesis, Xi'an Jiaotong University, Xi'an, Shanxi, China, 2003.
[2] Zhong Hongsheng, Pneumatic Transmission and Control, Beijing: China Machine Press, 1992, pp. 1~116.
[3] He Yue, Modern Control Theory Foundation, Beijing: China Machine Press, 1988, pp. 1~125.
[4] Hanchin G.D, Ozguner U and Drakunov S, "Nonlinear Control of a Rodless Pneumatic Servoactuator", Control Applications, 1992, pp. 516~521.
[5] Li Shiyong, Fuzzy control, Neural Network and Intelligent Control Theory, China: Harbin Institute of Technology press, 1998, pp. 8~19.
[6] Yang Gongjun, "Research on Pneumatic Intelligent Multi-point Position Control System", Beijing Institute of Technology, Beijing, China, 1995.
[7] Gan Chengyu, "Research on Control Method and Implementation of Pneumatic Pressure Loading System", Postgraduate dissertation, Xi'an Jiaotong University. Xi'an, Shanxi, China, 1995.
[8] Xu Hong and Tao Guoliang, "Theoretical Analysis on Damping Pressure-variable Proportional Servo System and Experimental Research on Its Lows-speed Features", China Mechanical Engineering, vol. 13, pp. 1280-1286, No.15, 2002.